UDC 621.313 https://doi.org/10.20998/2074-272X.2023.6.02

B. Larbi, M. Hatti, K. Kouzi, A. Ghadbane

Axial flux machine with non-slotted TORUS-NS rotor type. Design and investigate for electric traction

Introduction. *The drive electric motor is one of the key components in the traction chain of an electric vehicle. Traditional radial flux motors used in electric vehicles, which use permanent magnets or induction motors in an electric field, are experiencing significant development aimed at optimizing their weight and cost. However, it can only go so far, so switching to a completely different type of machine, such as an axial flow, might be a good alternative. The* ***novelty*** *to this item is an axial flux permanent magnet motorization with non-slotted TORUS-NS rotor (single interior stator with two external rotors North-South) type housed in the wheel of the vehicle; this allows power to pass directly from the motor to the wheel, increasing the efficiency of the motor. System complexity is also less, as the transmission, differentials and driveshaft are eliminated.* ***Purpose*** *is to equip the electric car and choose the motor adapted to the application and the available space. The smaller size and weight allows for a lighter vehicle and more batteries, thus increasing range. The focus on customization is because vehicle performance is so dependent on the quality of the vehicle architecture , battery pack and axial flux motor design. The* ***results*** *obtained are in good agreement of accuracy, in particular the flux density at the air gap. The investigation is carried out by the finite element method. Machine model was run on Maxwell 16.0 business code.* References 22, table 1, figures 10.

Key words: **axial flux permanent magnet machine, electric vehicle, finite element method, TORUS-NS.**

Вступ*. Привідний електродвигун є одним із ключових компонентів тягового кола електромобіля. Традиційні двигуни з радіальним магнітним потоком, що використовуються в електромобілях, в яких використовуються постійні магніти або асинхронні двигуни в електричному полі, переживають значний розвиток, спрямований на оптимізацію їхньої ваги та вартості. Однак це не межа, тому гарною альтернативою може бути перехід на зовсім інший тип машини, наприклад, з осьовим потоком.* ***Новизною*** *у цьому питанні є машина з постійним магнітом з осьовим магнітнім потоком та безпазовим ротором TORUS-NS (один внутрішній статор з двома зовнішніми роторами північ-південь), розміщеним у колесі транспортного засобу; це дозволяє потужності передаватися безпосередньо від двигуна до колеса, підвищуючи ефективність двигуна. Складність системи також знижується, оскільки відсутні трансмісія, диференціали та карданний вал.* ***Мета*** *полягає в тому, щоб обладнати електромобіль та вибрати двигун, адаптований до застосування та доступного простору. Найменші розмір і вага дозволяють використовувати більш легкий автомобіль та більше батарей, що збільшує пробіг. Особлива увага приділяється індивідуальному настроюванню, оскільки продуктивність автомобіля багато в чому залежить від якості його архітектури, акумуляторної батареї та конструкції двигуна з осьовим магнітним потоком. Отримані* ***результати*** *перебувають у добрій згоді за точністю, зокрема за густиною потоку у повітряному зазорі. Дослідження проводиться методом скінченних елементів. Модель машини була досліджена з використанням комерційного програмного продукту Maxwell 16.0.* Бібл. 22, табл. 1, рис. 10.

Ключові слова: **машина з постійним магнітом з осьовим потоком, електромобіль, метод скінченних елементів, електрична машина типу TORUS-NS.**

1. Introduction. Road transport is one of the biggest emitters of greenhouse gases in the world and one of the main sources of air pollution. Faced with this colossal challenge, the world has embarked on an ambitious transition policy towards cleaner and more efficient energy, improving performance, efficiency, safety and sustainability [1] with less polluting transport judged as a strong requirement. One of the solutions for reducing polluting gas emissions is the development of electric vehicles, while the traction of electric vehicles is entirely provided by electric motors. Unfortunately, electric vehicles have several disadvantages compared to internal combustion vehicles: for example; very limited autonomy, and high manufacturing costs.

On the might of these points, it is obvious that the motor for this vehicle must be very efficient. Due to its disc-shaped structure and high compactness, the topology of the axial flux permanent magnet (AFPM) machine is well suited for direct drive motor applications in the wheels [2]. Innovative solutions for emerging low-speed vehicles each providing a wide range of benefits in the areas these vehicles move through. The use of low-speed vehicles helps users enjoy the benefits of low-speed electric vehicles even more. For this purpose, a mode for low-speed vehicles was chosen for this study where the nominal speed of the wheels is 200 rpm.

The objective of this paper is to design the twin rotor axial flux synchronous motor without slot with internal stator (TORUS) according to the dimensioning equation. 3D finite element analysis is used for the accuracy of the electromagnetic air gap density.

2. Axial flux permanent magnet machine.

A. Presentation of the axial flux machine. A radial flux motor generates flux perpendicular to the axis of rotation, where the rotor is made of permanent magnets located inside a stator that contains support known as a yoke, which is outfitted with «teeth» containing electromagnetic coils that work as alternating magnetic poles. These poles interact with the alternating magnetic flux of the stator coils, which produces rotation of the rotor and therefore of the motor. An axial flux motor design has a different geometry from a radial machine, since its stator disc sandwiched between two rotor discs distinguishes the motor. In this design, the flux is generated parallel to the axis of rotation. This carries has the advantage of simplifying the fabrication of the motor (Fig. 1).

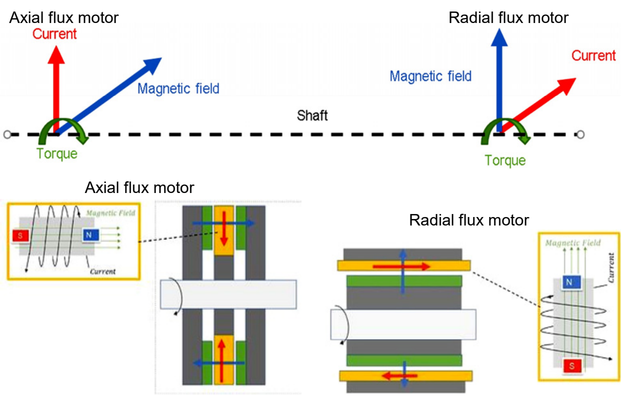

Fig. 1. Operating principles of the machine

B. Topologies of axial flux machines. Several axial flux machine configurations are shown in Fig. 2. Are classified into several categories [3, 4] according to:

- *construction*: number of stators and rotors, and their locations to each others.
- *winding support*: slotted, unslotted.
- *type of winding produced*: distributed, concentrated, Gramme ring.
- *arrangement of magnets*: on the surface, buried radially, buried tangentially.

Moreover, in literature, 4 main families are classified according to the type of structure:

1. «Single face» machine or a machine with 1 rotor and 1 stator.
2. «TORUS» (single interior stator with two external rotors) machine, where the stator is between 2 rotors.
3. «AFIR» (axial flux internal rotor) machine, where the rotor is between 2 stators.
4. Multi-stage machine with several stators and rotors.

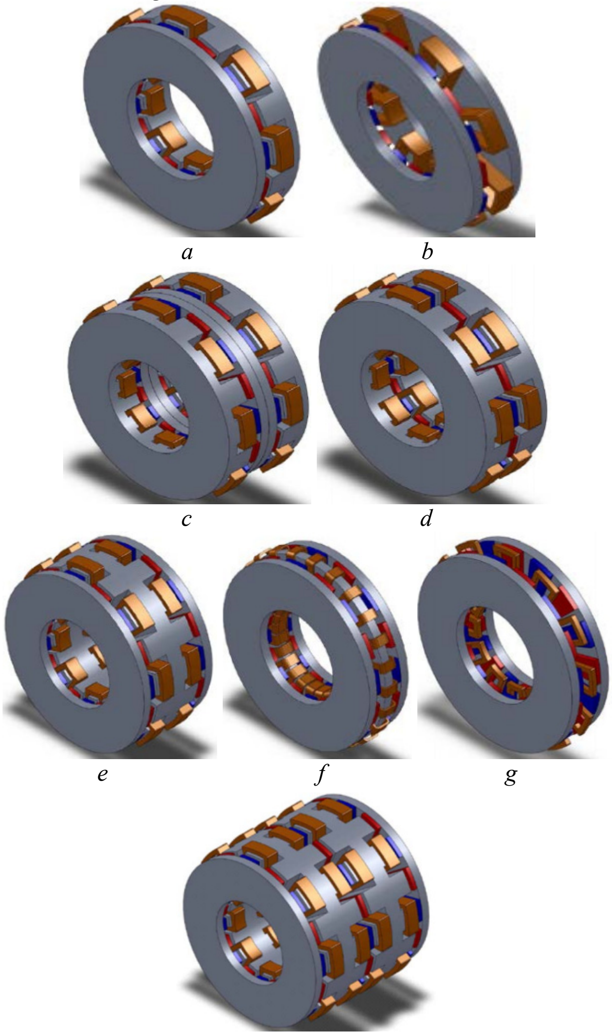

Fig. 2. AFPM synchronous motor topologies:
a, *b* – single stator-single rotor [5]; *c*, *d* – dual stator-single rotor; *e*, *f*, *g* – dual rotor-single stator; *h* – multistage structure

3. Geometrical modeling, and dimensioningof the AFPM machine.

A. Machine suitable for automotive application. In order to be able to select the best machine meeting the needs of our application, a small comparison between the different topologies of the AFPM machine illustrated in Fig. 2 is made to extract the advantages and disadvantages of each machine in order to be able to select the most suitable topology and meeting the different requirements of our application. Firstly, single air gap structures of the 1 stator/1 rotor type are eliminated in favor of multiple air gap structures because the objective is to have a mechanically balanced structure where the axial forces in operation compensate each other. In addition, a multiple air gap structure allows us to use a larger electromechanical conversion surface than the single air gap structure and, therefore, to hope to meet the performance required for our application. However, the reduced axial size imposed by the wheel and the obligation to work with discs of significant thickness prohibits multi-disc structures with more than two air gaps. The choice made among the symmetrical structures with two air gaps, we eliminate the structure with two stator and one rotor because of volume in favor of a structure with two rotor and one stator, therefore the selection remains between the TORUS-NN machine a magnetic flux emanates from a permanent magnet (PM), passes through the air gap, passes through the stator core and completes the circuit at the opposite polarity PM [6], stator and TORUS-NS or the direction of the flux changes such that the flux moves along the axis of the stator; in other words, the flux moves from the first rotor to the stator towards the second rotor without circulating along the stator yoke. In this case, the winding is placed on a disk of non-conductive and non-magnetic material [7], which implies a considerable reduction in iron losses and the elimination of the cogging torque which can be responsible for annoying torque ripples. Thus, this machine has a fairly advantageous mass torque [8]. In addition, the windings are placed at the level of the air gap and are in direct exposure to the magnetic field. At the end of this comparison and according to the criteria required for our application the TORUS machine where the stator is located between 2 mild steel rotors, carrying axially polarized magnets [9, 10] reaching relatively large dimensions air gap associated with a winding without an air gap [11]. The laminated stator strip wound toroid has a slotless toroidal winding that carries three phases. The geometric design of the TORUS-NS engine is shown in Fig. 3 [12]. The arrangement of the three-phase windings, the polarity of the magnet and the current path in the magnetic circuit through the diameter of the machine are shown in Fig. 4 [13].

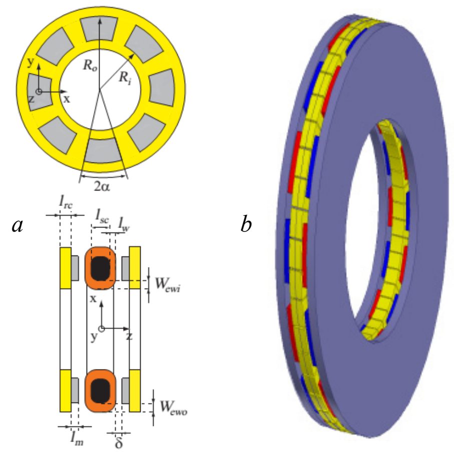

Fig. 3. *a* – definition of the geometrical parameters for the AFPM TORUS-NS motor [10]; *b* – configuration of the PM machine with axial flux TORUS without slot (TORUS-NS)

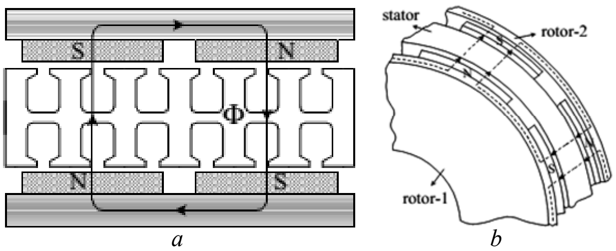

a *b*

Fig. 4. PM polarities and magnetic flux paths of a TORUS-NS machine [5]: *a* – 2D; *b* – 3D

B. Sizing equation for the AFPM machine. Two models of analytical modeling of electromagnetic phenomena are described, a simplified modeling was developed in order to set up dimensioning equations [14]. It is based on a reasoning on the power balance of the machine tha allows possibility to analyze, compare and pre-dimension machines of different structures. These models are fast, however, compromises must be made in terms of solution accuracy. The established sizing rules link input quantities such as geometry and power supply to output quantities which are the performance of these machines in terms of torque, losses, and efficiency. The sizing equations of machines with TORUS axial flow have the following form:

$$P_{out} = \eta \cdot \frac{m}{T} \cdot \int_0^T e(t) \cdot i(t) \mathrm{d}t = m \cdot K_p \cdot \eta \cdot E_{pk} \cdot I_{pk}, \quad (1)$$

where $e(t)$ is the electromotive force (EMF) due to PM; $i(t)$ is the supply current; E_{pk} is the maximum value of EMF in air gap; I_{pk} is the maximum value of current; K_p is the power coefficient; η is the motor efficiency; m is the phases number of motor [6, 15].

The power coefficient K_p is defined as:

$$K_p = \frac{1}{T} \cdot \int_0^T \frac{e(t) \cdot i(t)}{E_{pk} \cdot I_{pk}} \mathrm{d}t = \frac{1}{T} \cdot \int_0^T fe(t) \cdot fi(t) \mathrm{d}t. \quad (2)$$

The normalized EMF and current are defined as:

$$fe(t) = e(t) / E_{pk}; \quad fi(t) = i(t) / I_{pk}.$$

The form factor of the current is K_i defined as:

$$K_i = \frac{I_{pk}}{I_{rms}} = \left[\frac{1}{T} \cdot \int_0^T \left(\frac{i(t)}{I_{pk}} \right)^2 \mathrm{d}t \right]^{-0.5}, \quad (3)$$

where I_{rms} is the average square value of the phase current.

The maximum value of the phase air gap EMF for the AFPM in (1) is given as:

$$E_{pk} = K_e \cdot N_{ph} \cdot B_g \cdot \frac{f}{p} \left(1 - \lambda^2\right) \cdot D_0^2, \quad (4)$$

where K_e is the factor form voltage into account the type of winding; N_{ph} is the turns per phase number; B_g is the air gap magnetic flux density taken as a parameter to increase the mass moment [16]; f is the frequency of machine; p is the pole pairs number of machine; $\lambda = D_0 / D_0$, which is taken as a parameter to improve performance of motor [17]; D_0 is the outer diameter of motor; D_0 is the inside diameter of motor.

The maximum current value is given by:

$$I_{pk} = A \cdot \pi \cdot K_i \cdot \frac{1 + \lambda}{2} \cdot \frac{D_0}{2_{m1} \cdot N_{ph}}, \quad (5)$$

where m_1 is the number of phases in stator; A is the electrical load of machine.

Combining (1) to (5), we obtain measuring equation:

$$P_{out} = \frac{m}{m_1} \cdot \frac{\pi}{2} \cdot K_e \cdot K_p \cdot K_i \cdot A \cdot B_g \cdot \eta \cdot \frac{f}{p} \cdot \left(1 - \lambda^2\right) \cdot \left(\frac{1 + \lambda^2}{2} \right) \cdot D_0^3, \quad (6)$$

with introduction the aspect factor of the axial current machine [16]: $K_i = D_0 / L_e$, where L_e is the axial height of the machine, which is based on certain considerations of physical and geometrical quantities.

Using this parameter, second expression of the sixth dimensional equation (6) is deduced:

$$P_{out} = K_e \cdot K_i \cdot K_p \cdot K_L \cdot \eta \cdot B_g \cdot A \cdot \frac{f}{p} \cdot \left[\left(1 - \lambda^2\right) \cdot \frac{1 + \lambda}{2} \cdot D_0^2 \right] \cdot L_e. \quad (7)$$

The torque density of machine for total volume is:

$$\tau_{dem} = \frac{P_{out}}{w_m \cdot \frac{\pi}{4} \cdot D_{tot}^2 \cdot L_{tot}}, \quad (8)$$

where w_m is the angular speed of rotor; D_{tot} and L_{tot} are the total outer diameter and the total length of machine respectively, including the outer diameter winding end [2, 6, 17].

A general approximation of the size equation can be easily applied to TORUS surface-mounted PM motors [6]. The diameter of the outer surface D_0 can be specified as:

$$D_0 = \left(\frac{P_{out}}{\frac{\pi \cdot m}{2 \cdot m_1} \cdot K_e \cdot K_p \cdot K_i \cdot A \cdot B_g \cdot \eta \cdot \frac{f}{p} \cdot \left(1 - \lambda^2\right) \cdot \left(\frac{1 + \lambda}{2} \right)} \right)^{\frac{1}{3}}. \quad (9)$$

Axial height of active parts L_e (7) is expressed as a function of geometric and magnetic parameters of axial flux machine, the axial height of active parts can be expressed by:

$$L_e = L_s + 2 \cdot L_r + 2 \cdot g, \quad (10)$$

where L_r is the active length of the rotor:

$$L_r = L_{cr} + L_{PM}, \quad (11)$$

where L_{cr}, L_{PM} are the axial height of a rotor yoke and magnets respectively; g is the axial thickness of machine air gap; L_s is the height of the toroidal stator without notch. This height is made up of a laminated ferromagnetic yoke to height L_{cr}, and that of the windings in the axial direction, denoted W_{cu}:

$$L_s = L_{cs} + 2 \cdot W_{cu}. \quad (12)$$

In order to evaluate W_{cu} in [17] was developed a method based on volume considerations. By introducing the effective surface current density J_s in the copper wire, and the winding factor K_{cu} simple considerations on the volume of copper allow us to write that:

$$W_{cu} = \frac{D_i - \sqrt{D - \left(2 \cdot A \cdot D_g / K_{cu} \cdot J_s\right)}}{2}. \quad (13)$$

This size is also useful not only for the axial size, but also for radial dimensions, because it can then write the total exterior diameter of the machine in the form:

$$D_{tot} = D_0 + 2W_{cu}. \quad (14)$$

The thickness of the yoke of the stator is obtained as:

$$L_{cs} = \frac{B_g \cdot \pi \cdot \alpha_p \cdot D_0 \cdot (1 + \lambda)}{4 \cdot p \cdot B_{cs}}, \quad (15)$$

where B_{cs} is the flux density in the stator core.

For the rotor thickness, the previous expression must be divided by a factor of two, since the rotor yoke must only channel the magnetic flux present on one side:

$$L_{cr} = \frac{B_u \cdot \pi \cdot D_0 \cdot (1+\lambda)}{8 \cdot p \cdot B_{cr}}, \tag{16}$$

where B_u is the average magnetic flux density on a pole at surface of magnets. Axial height of magnets L_{PM} as function of maximal required magnetic flux density B_g is:

$$L_{PM} = \frac{K_f \cdot B_g}{B_r - \frac{1}{\beta_\alpha} \cdot B_u} \cdot (g + W_{cu}), \tag{17}$$

where β_α is the relative opening angle of the magnet with respect to the pole pitch; K_f is the ratio of the mean value of the air gap magnetic flux density under a pole B_u to its maximum value B_g [19], and must be determined by three-dimensional finite elements in the axial flux machine.

The form factor of an axial flux machine, whose expression [20]:

$$K_L = \frac{1}{\left[\begin{array}{l} \frac{\pi \cdot (1+\lambda)}{4 \cdot p} \left(\frac{K_f \cdot B_g}{B_{cs}} + \frac{B_u}{B_{cs}} \right) + \\ + \frac{1}{D_0} (2 \cdot W_{cu} + 2 \cdot g) \left(1 + \frac{K_f \cdot B_g}{B_r - \frac{1}{\beta_\alpha} \cdot B_u} \right) \end{array}\right]}. \tag{18}$$

C. 3D finite element modeling. The complexity of AFPM on surfaces with a single stator double rotor structure requires 3D finite element numerical analysis. In general, finite element modelling and simulation are used to take into account non-linear and three-dimensional aspects of electrical machines [21]. However, this type of simulation is becoming increasingly common in industry. Figure 5 shows the assembled machine using Ansys Maxwell 3D 16.0 Software (the machine design has been modelled here). Meshing is an important step in numerical modeling [22]. Improper meshing can lead to incorrect results. It is therefore important to develop a mesh in combination between smoothness and computation time. This machine was initially designed to meet the conditions for integration in the wheels of electric cars.

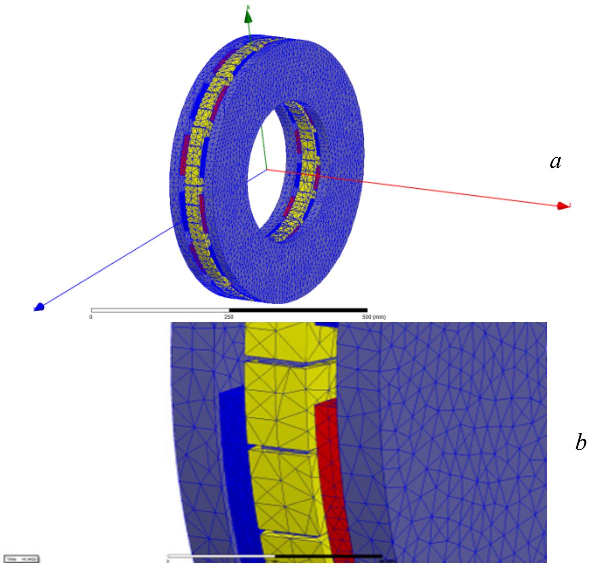

Fig. 5. Illustration and mesh of a double rotor axial magnet machine with internal stators TORUS-NS:
a – general geometry of machine; *b* – part of machine

The geometrical and electrical parameters are detailed in Table 1.

Table 1
Geometrical and electrical parameters of the TORUS-NS AFPM

Parameter	Value
Main voltage V_L, V	219.05
Phase voltage V_P, V	126.47
Number of pole pair p	14
Electrical loading A, A/m	10500
Current density J, A/mm^2	7.8
Air-gap flux density B_g, T	0.74
Diameter ratio λ	0.5745
Electrical power wave factor K_p	0.777
Current wave form factor K_i	0.134
EMF factor K_e	Π
Copper fill factor K_{Cu}	0.33
Residual magnetic flux density of PM material B_r, T	1.17
Leakage flux factor K_d	0.533
Specific magnetic loading B_u, T	1.125
Outside diameter D_o, mm	470
Internal diameter D_i, mm	270
Average diameter D_g, mm	370
Air-gap length g, mm	1.5
Flux density in the stator core B_{cs}, T	1.245
Axial span of the stator core L_{cs}, mm	20
Winding width at internal thickness W_{cui}, mm	5.5
Winding width at external diameter W_{cuo}, mm	3.2
Interior diameter along side width W_{cu}, mm	4.3
Stator core length L_s, mm	28.8
Rotor core length L_{cr}, mm	20
Magnet thickness-to-pole field ratio α_i	0.72
Average diameter magnet breadth WP_{Mg}, mm	29.9
Axial length of the rotor L_r, mm	32.7
Axial length of the machine L_e, mm	97
Number of winding turns per phase N_t	160
Phase current rms value I_{ef}, A	12.71
Axial thickness of the winding l_w, mm	4.4
Cross-section area of wire S_w, mm^2	0.396
Wire conductor diameter d_w, mm	0.71
Effective axial length of machine L_i, mm	100
Average length of the armature turn L_{1av}, mm	257.6
Nominal power P_R, W	5000
Number of phase m	3
DC voltage V_{DC}, V	210
Frequency f, Hz	46.67
Nominal speed, rpm	200
Connection	Y

Figure 6 in 3D model shows the distribution of magnetic flux density ***B*** of yoke vector distribution. In magnetic analysis, the motor is simulated at a certain time to obtain the magnetic field distribution. In this way, it is possible to check whether the design geometry is correct, by observing flux density distribution in air gap, in which central radius is obtained.

The results are shown in Fig. 7, 8.

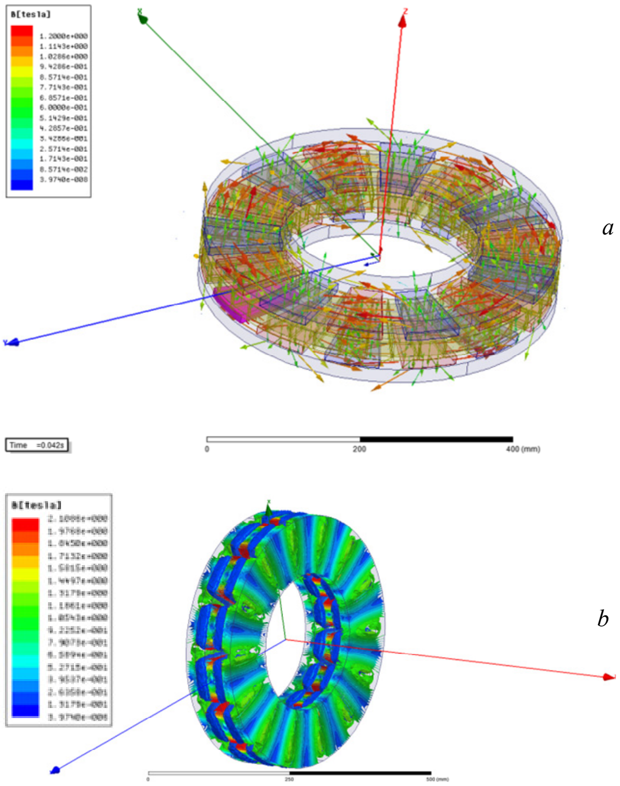

Fig. 6. *a* – magnetic field strength with vectors;
b – magnetic flux density distribution in the motor

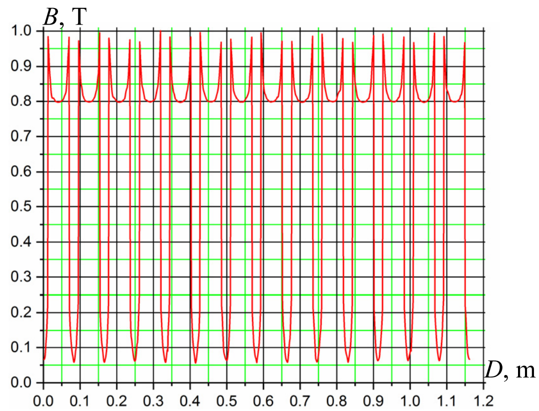

Fig. 7. Air gap flux density magnetic distribution for average radius (average diameter $D_g = (D_i + D_o)/2$)

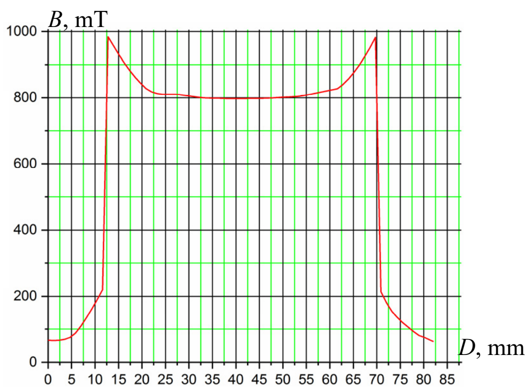

Fig. 8. TORUS-NS air gap flux densityunder one pole

The expositions of the stator core and rotor to time-varying flux densities were studied. The results are illustrated in Fig. 9, 10.

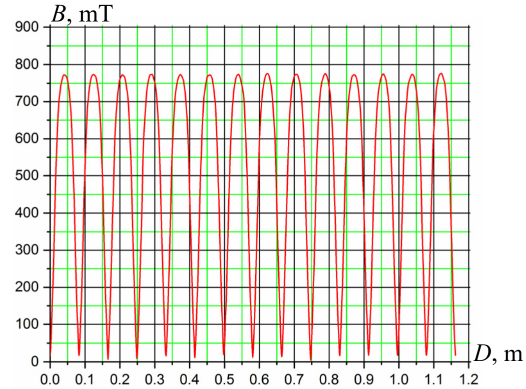

Fig. 9. Stator yoke flux density magnetic distribution for average radius

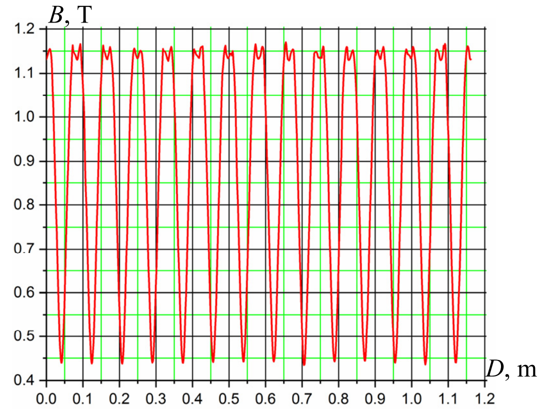

Fig. 10. Rotor yoke flux density magnetic distribution for average radius

4. Conclusions. The current global context has prompted car manufacturers to electrify their vehicles. In order to reduce the cost, which is still high, various technical solutions need to be implemented in these types of vehicles to reduce the cost of the power-train/electric transmission components, particularly the electric machines.The main objective of this article is to study an electric machine that can satisfy severe constraints in terms of performance and size for an application in a direct drive system for electric vehicles.

It is important to achieve optimum performance: high torque density with maximum efficiency over a wide speed range, which would impact the use of analytical models based on the sizing equationsin order to identify the best geometry of the machines application. Therefore, at the end of this study, axial flux machine with non-slotted TORUS-NS rotor type was selected due to its advantages. The numerical results using finite elements have given satisfied resukts to evaluate the potential of this machine.

For further study this machine, three-dimensional features are considered using the Maxwell Ansys finite element model. The results concerning the magnetic flux density in the air gap, obviousmy shown that it is necessary to improve the overall operation: in the end wheel motors begin to make their way to the automobile.

The effect of buried permanent magnet axially in the rotor has been planned as a perspective task and radial split of each permanent magnet into small pieces.

Conflict of interest. The authors declare that they have no conflicts of interest.

REFERENCES

1. Lasocki J., Krawczyk P., Kopczyński A., Roszczyk P., Hajduga A. Analysis of the strategies for managing extended-range electric vehicle powertrain in the urban driving cycle. *Electrical Engineering & Electromechanics*, 2022, no. 1, pp. 70-76. doi: https://doi.org/10.20998/2074-272X.2022.1.10.

2. Caricchi F., Crescimbini F., Mezzetti F., Santini E. Multi-stage axial-flux PM machine for wheel direct drive. *IAS '95. Conference Record of the 1995 IEEE Industry Applications Conference Thirtieth IAS Annual Meeting*, 1995, vol. 1, pp. 679-684. doi: https://doi.org/10.1109/IAS.1995.530365.

3. Vun S.T., McCulloch M.D. Optimal Design Method for Large-Scale YASA Machines. *IEEE Transactions on Energy Conversion*, 2015, vol. 30, no. 3, pp. 900-907. doi: https://doi.org/10.1109/TEC.2015.2397342.

4. Fan J., Lee Y. Sensorless control of switched reluctance motor based on a simple flux linkage model. *Electrical Engineering & Electromechanics*, 2023, no. 3, pp. 36-39. doi: https://doi.org/10.20998/2074-272X.2023.3.05.

5. Si J., Zhang T., Hu Y., Gan C., Li Y. An Axial-Flux Dual-Rotor Slotless Permanent Magnet Motor With Novel Equidirectional Toroidal Winding. *IEEE Transactions on Energy Conversion*, 2022, vol. 37, no. 3, pp. 1752-1763. doi: https://doi.org/10.1109/TEC.2021.3138465.

6. Patel A.N. Slot opening displacement technique for cogging torque reduction of axial flux brushless DC motor for electric two-wheeler application. *Electrical Engineering & Electromechanics*, 2023, no. 2, pp. 7-13. doi: https://doi.org/10.20998/2074-272X.2023.2.02.

7. Jacekf G., Rong W., Maarten K. *Axial Flux Permanent Magnet Brushless Machines. 2nd Ed.* Springer, 2008.

8. Caricchi F., Crescimbini F., Honorati O. Low-cost compact permanent magnet machine for adjustable-speed pump application. *IEEE Transactions on Industry Applications*, 1998, vol. 34, no. 1, pp. 109-116. doi: https://doi.org/10.1109/28.658730.

9. Gonzalez-Lopez D.A., Tapia J.A., Wallace R., Valenzuela A. Design and Test of an Axial Flux Permanent-Magnet Machine With Field Control Capability. *IEEE Transactions on Magnetics*, 2008, vol. 44, no. 9, pp. 2168-2173. doi: https://doi.org/10.1109/TMAG.2008.2000543.

10. Abu Ibaid O.Z.I., Belhamdi S., Abid M., Chakroune S., Mouassa S., Al-Sagar Z.S. Wavelet packet analysis for rotor bar breakage in an inverter induction motor. *Electrical Engineering & Electromechanics*, 2023, no. 3, pp. 3-11. doi: https://doi.org/10.20998/2074-272X.2023.3.01.

11. Profumo F., Zheng Zhang, Tenconi A. Axial flux machines drives: a new viable solution for electric cars. *IEEE Transactions on Industrial Electronics*, 1997, vol. 44, no. 1, pp. 39-45. doi: https://doi.org/10.1109/41.557497.

12. Liu C.-T., Lee S.-C. Magnetic field modeling and optimal operational control of a single-side axial-flux permanent magnet motor with center poles. *Journal of Magnetism and Magnetic Materials*, 2006, vol. 304, no. 1, pp. e454-e456. doi: https://doi.org/10.1016/j.jmmm.2006.02.065.

13. Gholamian S.A., Ardebil M., Abbaszadeh K., Mahmodi Charati S. Optimum Design of 1 kW Axial Flux Permanent Magnet Slotted TORUS Motor. *European Journal of Scientific Research*, 2008, vol. 21, no. 3, pp. 488-499.

14. Dlala E. Comparison of Models for Estimating Magnetic Core Losses in Electrical Machines Using the Finite-Element Method. *IEEE Transactions on Magnetics*, 2009, vol. 45, no. 2, pp. 716-725. doi: https://doi.org/10.1109/TMAG.2008.2009878.

15. Gholamian S.A., Ardebili M., Abbaszadeh K. Analytic and FEM evaluation of power density for various types of double-sided axial flux slotted PM motors. *International Journal of Applied Engineering Research (IJAER)*, 2008, vol. 3, no. 7, pp. 927-939.

16. Aydin M., Huang S., Lipo T.A. Optimum design and 3D finite element analysis of nonslotted and slotted internal rotor type axial flux PM disc machines. *2001 Power Engineering Society Summer Meeting. Conference Proceedings (Cat. No.01CH37262)*, 2001, vol. 3, pp. 1409-1416. doi: https://doi.org/10.1109/PESS.2001.970283.

17. Huang Y., Zhu J., Guo Y., Hu Q. Development of a High-Speed Claw Pole Motor with Soft Magnetic Composite Core. *2007 IEEE International Electric Machines & Drives Conference*, 2007, pp. 1564-1568. doi: https://doi.org/10.1109/IEMDC.2007.383661.

18. Surong Huang, Jian Luo, Leonardi F., Lipo T.A. A comparison of power density for axial flux machines based on general purpose sizing equations. *IEEE Transactions on Energy Conversion*, 1999, vol. 14, no. 2, pp. 185-192. doi: https://doi.org/10.1109/60.766982.

19. Jiang C., Qiao M., Zhu P., Zheng Q. Design and Verification of High Speed Permanent Magnet Synchronous Motor for Electric Car. *2018 2nd IEEE Advanced Information Management,Communicates,Electronic and Automation Control Conference (IMCEC)*, 2018, pp. 2371-2375. doi: https://doi.org/10.1109/IMCEC.2018.8469398.

20. Aydin M., Huang S., Lipo T.A. Axial flux permanent magnet disc machines: A review. *Conf. Record of SPEEDAM*, 2004, vol. 8, pp. 61-71.

21. Yatchev I., Balabozov I., Hinov K., Hadzhiev I., Gueorgiev V. Influence of the shape of the input pulses on the characteristics of hybrid electromagnetic system with magnetic flux modulation. *Electrical Engineering & Electromechanics*, 2021, no. 3, pp. 3-7. doi: https://doi.org/10.20998/2074-272X.2021.3.01.

22. Belkacem L., Mustapha H., Katia K., Ahmed G. Design and Investigation of Axial Flux Permanent Magnet Synchronous Machine for electric vehicles. *2018 International Conference on Communications and Electrical Engineering (ICCEE)*, 2018, pp. 1-6. doi: https://doi.org/10.1109/CCEE.2018.8634529.

Received 04.03.2023
Accepted 10.07.2023
Published 02.11.2023

Belkacem Larbi [1, 2]*, PhD,*
Mustapha Hatti [3]*, Professor,*
Katia Kouzi [2]*, Doctor,*
Ahmed Ghadbane[1]*, Doctor,*
[1] Nuclear Research Center of Birnie,
p.o. box 180 Ain Oussera, Algeria,
e-mail: l.belkacem.eln@lagh-univ.dz (Corresponding Author);
ghadbane_ahmed12@yahoo.com
[2] University Amar Telidji, Laghouat, Algeria,
e-mail: k.kouzi@lagh-univ.dz
[3] Solar Equipments Development Unit, UDES/CDER,
B.P. 386, 42004, Bou Ismail, Tipasa, Algeria,
e-mail: musthatti@ieee.org

How to cite this article:
Larbi B., Hatti M., Kouzi K., Ghadbane A. Axial flux machine with non-slotted torus-ns rotor type. Design and investigate for electric traction. *Electrical Engineering & Electromechanics*, 2023, no. 6, pp. 10-15. doi: https://doi.org/10.20998/2074-272X.2023.6.02